Neurobiology of Stress 18 (2022) 100453

Contents lists available at ScienceDirect

Neurobiology of Stress

journal homepage: www.elsevier.com/locate/ynstr

Repeated vagus nerve stimulation produces anxiolytic effects via upregulation of AMPAR function in centrolateral amygdala of male rats

Shao-Qi Zhang [a], Zhi-Xuan Xia [a], Qiao Deng [a], Ping-Fen Yang [a], Li-Hong Long [a,b,c,d,e], Fang Wang [a,b,c,d,e,**], Jian-Guo Chen [a,b,c,d,e,*]

[a] Department of Pharmacology, Tongji Medical College, Huazhong University of Science and Technology, Wuhan City, Hubei, 430030, China
[b] The Research Center for Depression, Tongji Medical College, Huazhong University of Science and Technology, 430030, Wuhan, China
[c] The Key Laboratory for Drug Target Researches and Pharmacodynamic Evaluation of Hubei Province, 430030, Wuhan, China
[d] Key Laboratory of Neurological Diseases (HUST), Ministry of Education of China, Wuhan, Wuhan City, Hubei, 430030, China
[e] Laboratory of Neuropsychiatric Diseases, The Institute of Brain Research, Huazhong University of Science and Technology, 430030, Wuhan, China

ARTICLE INFO

Keywords:
AMPAR
Anxiolytic effects
Centrolateral amygdala
rVNS
β-adrenergic receptors

ABSTRACT

Repeated vagus nerve stimulation (rVNS) exerts anxiolytic effect by activation of noradrenergic pathway. Centrolateral amygdala (CeL), a lateral subdivision of central amygdala, receives noradrenergic inputs, and its neuronal activity is positively correlated to anxiolytic effect of benzodiazepines. The activation of β-adrenergic receptors (β-ARs) could enhance glutamatergic transmission in CeL. However, it is unclear whether the neurobiological mechanism of noradrenergic system in CeL mediates the anxiolytic effect induced by rVNS. Here, we find that rVNS treatment produces an anxiolytic effect in male rats by increasing the neuronal activity of CeL. Electrophysiology recording reveals that rVNS treatment enhances the alpha-amino-3-hydroxy-5-methyl-4-isoxazole propionic acid receptor (AMPAR)-mediated excitatory neurotransmission in CeL, which is mimicked by β-ARs agonist isoproterenol or blocked by β-ARs antagonist propranolol. Moreover, chemogenetic inhibition of CeL neurons or pharmacological inhibition of β-ARs in CeL intercepts both enhanced glutamatergic neurotransmission and the anxiolytic effects by rVNS treatment. These results suggest that the amplified AMPAR trafficking in CeL via activation of β-ARs is critical for the anxiolytic effects induced by rVNS treatment.

1. Introduction

Anxiety disorders are among the common class of neuropsychiatric diseases, with a lifetime prevalence of more than 28% (Calhoon and Tye, 2015; Craske and Stein, 2016). Moreover, anxiety disorders are still thought to be largely complicated due to the high co-morbidity with other psychiatric disorders, such as major depression and substance abuse, indicating the need for developing new treatment for anxiety disorders based on its neurobiological mechanisms.

Recently, both preclinical and clinical studies demonstrate that repeated vagus nerve stimulation (rVNS) treatment reduces anxiety (Furmaga et al., 2011; George et al., 2008; Noble et al., 2019; Rush et al., 2000; Shah et al., 2016). However, the neurobiological mechanisms underlying the anxiolytic action of rVNS remain unclear. The projection of vagal afferents to the nucleus of solitary tract (NTS) is important to understand how vagal activation may affect anxiety-like behaviors. The NTS is the termination of vagal primary afferent, which sends direct and indirect ascending projections to emotion-related brain areas, such as amygdala, locus coeruleus (LC), and hippocampus (Berthoud and Neuhuber, 2000; Jia et al., 1997; Ricardo and Koh, 1978). The central amygdala (CeA) is known to be highly innervated by noradrenergic afferents. Previous studies have demonstrated that CeA receives noradrenergic inputs from NTS and LC (Campese et al., 2017; Chen et al., 2019; Gu et al., 2020), and the ascending noradrenergic system to CeA has been reported to be involved in fear conditioning and stress responses (Khoshbouei et al., 2002). Furthermore, the noradrenergic system has also been shown to be critical in rVNS anxiolytic effect (Furmaga et al., 2011). Therefore, we wondered whether the

* Corresponding author. Department of Pharmacology, Tongji Medical College, Huazhong University of Science and Technology, 13 Hangkong Road, Wuhan, Hubei, 430030, China.
** Corresponding author. Department of Pharmacology, Tongji Medical College, Huazhong University of Science and Technology, Wuhan City, Hubei, 430030, China.
E-mail addresses: wangfangtj0322@163.com (F. Wang), chenj@mails.tjmu.edu.cn (J.-G. Chen).

https://doi.org/10.1016/j.ynstr.2022.100453
Received 1 October 2021; Received in revised form 27 March 2022; Accepted 18 April 2022
Available online 22 April 2022

noradrenergic system in CeA contributed to rVNS-induced anxiolytic effect.

Noradrenaline (NE) is an important neurotransmitter in the central nervous system and regulates glutamatergic neurotransmission in brain regions involved in emotional response (Faber et al., 2008; Luo et al., 2015). The brain NE level displays an intensity-dependent transient increase in response to VNS (Roosevelt et al., 2006). Alpha-amino-3-hydroxy-5-methyl-4-isoxazole propionic acid receptor (AMPAR) confers rapid conductance and permeability properties, which is known to be critical for glutamatergic synaptic plasticity and stress response. Recent study has reported that NE facilitates the synaptic delivery of GluA1-containing AMPARs in hippocampus (Hu et al., 2007). Consistent with this observation, our previous study has demonstrated that NE, via activation of β-adrenergic receptors (β-ARs), enhances the surface expressions of GluA1 subunit-containing AMPA receptors and synaptic plasticity in hippocampus, and then ameliorates the emotional memory deficits in aged rats (Luo et al., 2015). Glutamatergic neurotransmission in CeA is critical for anxiety-like behaviors (Beitchman et al., 2019; Natividad et al., 2017). The CeA, which is encompasses the centrolateral (CeL) and centromedial (CeM) subdivision, is an essential hub for anxiety processing. CeL GABAergic neurons control behavioral responses to stress by inhibitory inputs to CeM, which serves as CeA output (Duvarci and Pare, 2014; Janak and Tye, 2015; Tye and Deisseroth, 2012). Several reports have demonstrated that benzodiazepines produce anxiolytic activity through activation of CeL neurons (Carvalho et al., 2012; Griessner et al., 2018). In particular, previous evidence demonstrates that infusion of CeL with the AMPAR antagonist induces anxiety-like behaviors (Tye et al., 2011). Additionally, β-ARs agonist isoproterenol increases glutamatergic neurotransmission in CeL (Silberman and Winder, 2013). Accordingly, we asked whether the action of noradrenergic system on excitatory neurotransmission in CeL contributed to rVNS-induced anxiolytic-like behaviors.

In the present study, using combined electrophysiological, biochemical, pharmacological, and chemogenetic approaches, as well as behavioral studies, we demonstrated that rVNS treatment produced the anxiolytic action, and found that activation of noradrenergic system promoted AMPAR-mediated excitatory neurotransmission in the CeL neurons, and then increased inhibitory inputs into CeM output neurons, contributing to the anxiolytic action induced by rVNS. These findings provide a novel therapeutic strategy for anxiety disorders.

2. Materials and methods

2.1. Animals

Male Sprague-Dawley rats (200–250 g) were housed in groups of two to four per cage, and maintained under standard laboratory conditions (12-h light/dark cycle and constant temperature (22 ± 2 °C)) with free access to water and food, unless otherwise indicated. All experimental protocols complied with the National Institutes Guide for the Care and Use of Laboratory Animals and approved by the Animal Welfare Committee of Huazhong University of Science and Technology.

2.2. Implantation of vagal nerve stimulators

Surgical procedure was carried out as previously described with minor modifications (Furmaga et al., 2011). Rats were anesthetized with sodium pentobarbital (40 mg/kg) by intraperitoneal injection (i.p.), and coil electrodes were placed around the left cervical vagus nerve and connected to the two-channel connector that affixed to the nape. Following implantation, cessation of breathing was visually monitored and evaluated for correct implantation and effectiveness of the VNS cuff, through applied with current stimulation (0.8 mA, 1 s) under anesthesia. Seven days after surgery, the rVNS group was instrumented with an operational stimulator (Chengdu instrument factory, Chengdu, China) that was programed by a handheld computer, and received treatment for 6 days. The stimulation paradigm consisted of 0.5 mA current, 500 μs pulse width at 30 Hz, stimulation cycle of 30 s on and 5 min off. Sham-operated rats were treated in the same manner except that no stimulation was performed.

2.3. Complete subdiaphragmatic vagotomy (SDV)

Rats were maintained on a liquid diet for at least 3 d and food-deprived for one day before surgery to promote survival and recovery. Rats were anesthetized with sodium pentobarbital (40 mg/kg, i.p.) and the abdominal midline incision was made. The connective tissue and overlying vasculature surrounding by the cardia were carefully isolated. The stomach was towed to expose the esophagus, and then the dorsal and ventral vagal trunks were exposed by gently teasing and isolated from the esophagus. The vagal trunks were resected and cauterized. Control rats received a sham surgery that consisted all surgical procedures except for the resection and cauterization of the vagus nerve. Before rVNS, SDV was verified functionally with intraperitoneal cholecystokinin (CCK-8, 2 μg/kg, i.p., TGpeptide, 127P03, Nanjing, China)-induced food intake reduction as described previously (Davis et al., 2020).

2.4. Behavioral tests

After treatment with rVNS, rats were subjected to behavioral tests. Anxiety-like behaviors were evaluated sequentially with open field test (OFT), elevated plus maze (EPM) and novelty suppressed feeding test (NSFT). After that, depression-like behaviors were assessed by sucrose preference test (SPT) and forced swim test (FST). The details about SPT and FST are provided in the supplementary information.

2.4.1. Open field test

The OFT was monitored in a plastic arena (100 cm (w) × 100 cm (d) × 40 cm (h)). The rat was gently placed into the center zone and allowed to explore for 5 min. ANY-maze behavioral tracking system (Stoelting Co. New Jersey, USA) was used to record the process: the total distance traveled as a measure of locomotor activity, the entries, duration, and distance in the central zone were assessed as an anxiolytic indicator.

2.4.2. Elevated plus maze

EPM was performed as previously described with modifications (Shen et al., 2019). The instrument contained a 10 cm × 10 cm central square, two open arms and two closed arms at 50 cm × 10 cm each. The closed arms had a black wall of 30 cm in height. Each rat was placed in the central square with its head toward the closed arm. The number of entries, the time spent in the open arms, and distance in the open arms were recorded over a period of 5 min using ANY-maze behavioral tracking system.

2.4.3. Novelty suppressed feeding test

The NSFT was carried out as described by a previous study with minor modification (Zhang et al., 2018). Rats were fasting for 24 h before the experiment. 1 h before testing, rats were transferred to the test room. Food pellets were placed on a piece of paper positioned in the center of 100 cm × 100 cm × 40 cm open field apparatus. Rats were placed individually in the corner, facing the center zone. The latency to feed was monitored for a maximum period of 8 min by the ANY-maze behavioral tracking system. Food consumption was recorded during the test and 30 min after the test.

2.5. Electrophysiological recording

Rats were anesthetized with sodium pentobarbital (40 mg/kg, i.p.) and perfused with ice-cold oxygenated cutting solution containing (mM): sucrose 209, ascorbic acid 11.6, sodium pyruvate 3.1, $MgSO_4$ 4.9, $NaHCO_3$ 26.2, NaH_2PO_4 1.0, glucose 20, pH 7.4, osmolarity 290–310

mOsm. Brain slices were incubated in artificial cerebrospinal fluid (ACSF) containing (mM): NaCl 119, $MgSO_4$ 1.3, KCl 4.3, $NaHCO_3$ 26.2, NaH_2PO_4 1.0, glucose 10, $CaCl_2$ 2.9, pH 7.4, osmolarity 290–310 mOsm for recovery at 28 °C for 1 h. CeA-containing Slice was then transferred into the recording chamber with continuous perfusion of ACSF at room temperature. The rate of perfusion was 2 ml/min. The resistance of patch pipettes was 3–6 MΩ. For voltage-clamp recording, the internal solution contained (mM): $CsCl_2$ 140, HEPES 10, EGTA 0.2, $MgCl_2$ 1, ATP-Mg 4, GTP-Na_2 0.3, QX314 5, pH 7.2, osmolarity 290–310 mOsm for AMPAR-mediated miniature excitatory postsynaptic currents (mEPSCs), and the internal solution contained (mM): K-gluconate 140, NaCl 8, $MgCl_2$ 2, EGTA 1, HEPES 10, Mg-ATP 2 and Na-GTP 0.3, pH 7.2, osmolarity 290–310 mOsm for miniature inhibitory postsynaptic currents (mIPSCs). The mEPSCs on CeL neurons were observed by holding the cell at −70 mV with 20 μM bicuculline (Sigma-Aldrich, Saint Louis, USA) and 1 μM tetrodotoxin (Hebei Institute of Fisheries Science, Qinhuangdao, China) adding to the extracellular solution. The mIPSCs on CeA neurons was observed by holding the cell at −70 mV with 1 μM tetrodotoxin and 20 μM 6-cyano-7-nitroquinoxaline-2,3-dione (CNQX) (Sigma-Aldrich, Saint Louis, USA) and 30 μM D-2-amino-5-phosphonovalerate (AP-5) (Sigma-Aldrich, Saint Louis, USA) adding to the extracellular solution. For noradrenergic receptor agonist or antagonist manipulation, 10 μM of β-ARs agonist isoproterenol (Sigma-Aldrich, Saint Louis, USA), 50 μM of α-adrenergic receptor antagonist phentolamine (Sigma-Aldrich, Saint Louis, USA), and 10 μM of β-ARs antagonist propranolol (Sigma-Aldrich, Saint Louis, USA) dissolved in ACSF. After bath application for 10 min, whole-cell recordings were performed separately.

For current-clamp recording, we recorded action potentials (APs) of CeL neurons with the injection current of 0–140 pA at a holding potential of −70 mV. The internal solution that contained (in mM), K-gluconate 97, KCl 38, EGTA 0.35, HEPES 20, NaCl 6, Phosphocreatine-Na 7, Mg-ATP 4, Na-GTP 0.35, pH 7.2, 280–300 mOsm for AP. All recordings were performed under an upright Olympus microscope (BX51WIF, Olympus, Tokyo, Japan). Signals were digitized at 10 kHz, filtered at 5 kHz and obtained through a MultiClamp 700B amplifier (Molecular Devices, Sunnyvale, CA) and acquired with pCLAMP10 software (Axon instruments, Molecular Devices, San Jose, CA). Series resistance was monitored during recording and data were discarded for those altered by $>$ 20%. Data were analyzed by the Mini Analysis Program (Synaptosoft, Decatur, GA, USA).

2.6. Stereotaxic injections and cannulas implantation

Rats were anesthetized with sodium pentobarbital (40 mg/kg, i.p.) and then fixed on a stereotactic apparatus. Designer receptor exclusively activated by designer drug (DREADD) virus: a viral cocktail (1:1) of AAV2-hSyn-Cre-pA (titers: 2.51×10^{12} VG/ml) mixed with AAV2-EF1α-DIO-hM4D(Gi)-mCherry virus (titers: 5.42×10^{12} VG/ml) or AAV2-hSyn-Cre-pA (titers: 2.51×10^{12} VG/ml) mixed with AAV2-EF1α-DIO-mCherry (titers: 3.98×10^{12} VG/ml) (BrainVTA, Wuhan, China) was bilaterally injected into the CeL (AP = −2.25 mm, ML = ±4.4 mm, DV = −8.3 mm; relative to bregma). The skull above the target area was drilled and 300 nl virus into each location at the rate of 30 nl/min. After completion of the injection, the needle was stayed for an additional 10 min and then slowly withdrawn. After recovering from four weeks, rats were intraperitoneally injected with clozapine-N-oxide (CNO) (5 mg/kg) (Griessner et al., 2018) 30 min before the rVNS program and behavioral tests were carried out.

For intra-CeL microinjection, 22-gauge stainless steel guide cannulas (RWD Life Science, Shenzhen, China) were implanted bilaterally into the CeL. After the implantation surgery, rats were recovered for 7 days before further experiments. Propranolol (Sigma-Aldrich, Saint Louis, USA) was dissolved in ACSF (vehicle). CNQX (Sigma-Aldrich, Saint Louis, USA) was dissolved in 0.1% DMSO. These drugs including propranolol (10 μM) (Zhou et al., 2015), CNQX (20 μM, an electrophysiological dosage), and vehicle were microinjected into the CeL 30 min before rVNS.

2.7. Biotinylation of surface proteins and Western blot analysis

Tissue preparation and western blotting were performed according to our previous study (Zhou et al., 2019). The CeL slices from two rats were rinsed with ice-cold ACSF and then incubated with ACSF containing 1.0 mg/ml sulfo–NHS–LC-biotin (Thermo Fisher Scientific, Rockford, USA) for 90 min at 4 °C with gentle shaking. Unreacted reagent was removed by quenching with ACSF containing 100 mM glycine. After biotin incubation, protein extracts were prepared in ice-cold RIPA buffer. The protein concentration of each lysate was then quantified and equal weight of protein was incubated overnight with NeutrAvidin coupled-agarose beads (Thermo Fisher Scientific, Rockford, USA). Biotinylated surface proteins or total proteins were separated through 10% SDS-PAGE and transferred into nitrocellulose membranes (Millipore, MA, USA). The transferred membranes were then incubated overnight at 4 °C with various primary antibody against GluA1 (1:1000 dilution; Abcam, ab31232, Cambridge, UK), GluA2 (1:1000 dilution; Abcam, ab52932, Cambridge, UK), NR2A (1:500 dilution; Abcam, ab124913, Cambridge, UK), NR2B (1:500 dilution; Abcam, ab65783, Cambridge, UK), and β-actin (1:3000 dilution; Santa Cruz Biotechnology, A1978, Dallas, TX, USA). After washing three times, bands were incubated in the horseradish peroxidase-conjugated secondary antibodies and then visualized by the MicroChemi (DNR Bio-imaging systems, Jerusalem, Israel). Protein levels were quantified by using the ImageJ software (NIH, MD, USA). The surface protein (s) level was normalized to its total protein (t), and total protein level was normalized to β-actin loading control (Carmichael et al., 2018; Fan et al., 2019).

2.8. Immunohistochemistry

The rats were anesthetized with sodium pentobarbital (40 mg/kg, i.p.) and then transcardially perfused with saline followed by 4% paraformaldehyde (PFA). Brains were dissected out, post-fixed in 4% PFA overnights at 4 °C, and then transferred to 30% sucrose at 4 °C until sinking. Frozen coronal sections (40 μm thick) containing the CeA were obtained by a cryostat microtome (CM1900, Leica, Wetzlar, Germany). The sections were incubated with primary antibody overnight at 4 °C. The primary antibodies included: rabbit anti-c-Fos (1:1000 dilution; Abcam, ab208942, Cambridge, UK) and mouse anti-ΔFosB antibody (1:1000 dilution; Cell Signaling Technology, 14695, Denvars, MA, USA). Sections were then incubated with secondary antibodies of Alexa Fluor 488 Donkey anti-Mouse IgG (H + L) antibody (1:800 dilution; Invitrogen, A21206, Paisley, UK) and Alexa Fluor 594 Donkey anti-Mouse IgG (H + L) antibody (1:800 dilution; Invitrogen, A21203, Paisley, UK). Images were acquired via a laser confocal scanning microscope (FV1000, Olympus, Tokyo, Japan). The number of c-Fos and ΔFosB positive cells in CeL, CeM, and the entire NTS were counted with ImageJ software (NIH, MD, USA).

2.9. Statistical analysis

All data were presented as the mean ± SEM and performed in GraphPad Prism 8.0 software (GraphPad, San Diego, CA, USA). Comparison between two groups was evaluated by unpaired Student's *t*-test. Multiple comparisons were carried out using one-way or two-way analysis of variance (ANOVA) followed by Bonferroni's post hoc test. $p < 0.05$ were considered as statistical significance. The details are provided in the supplementary information.

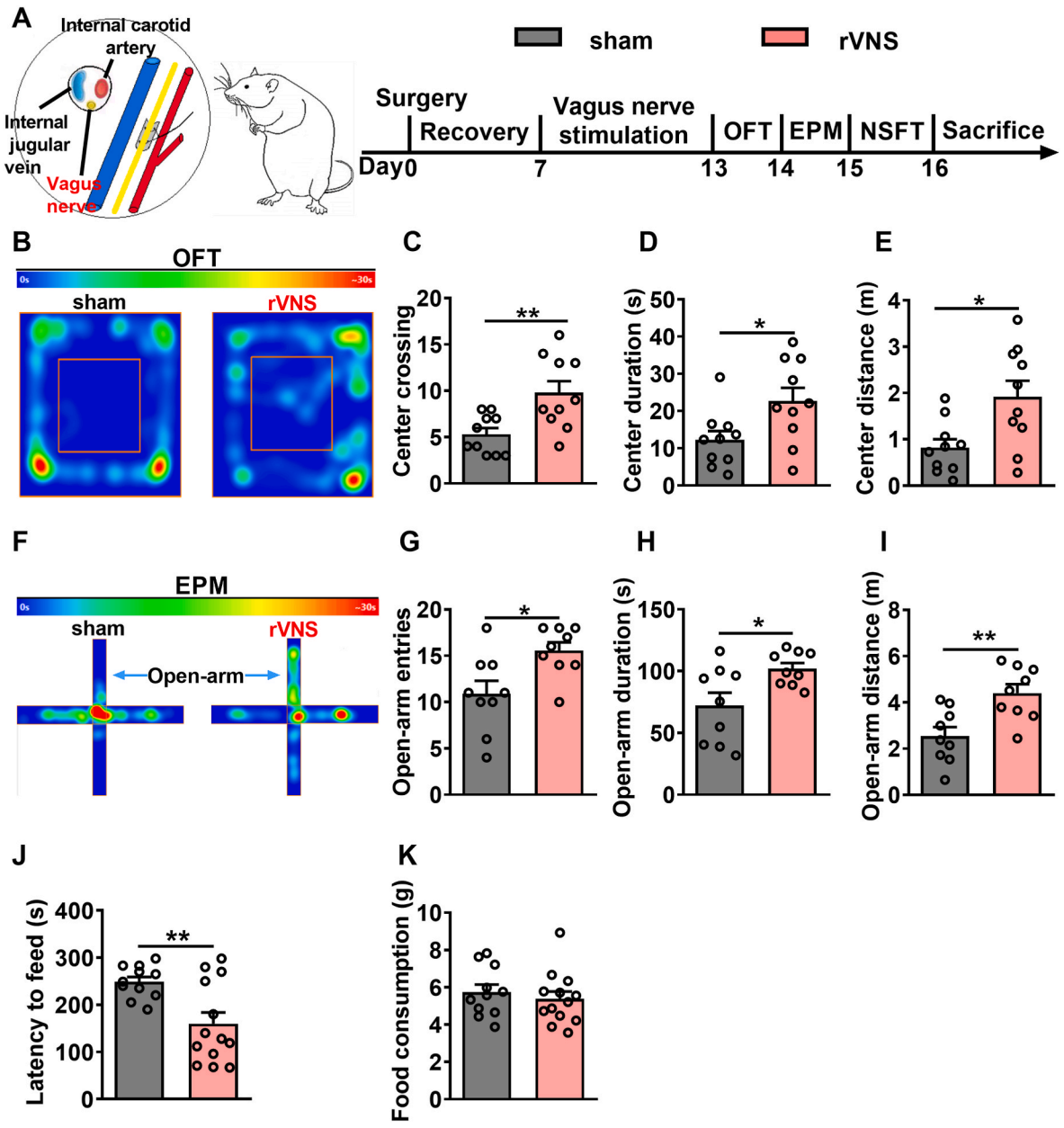

Fig. 1. Repeated vagus nerve stimulation induces anxiolytic-like behaviors in male rats. **(A)** The experimental drawing of vagus nerve stimulation (VNS) surgery (left), schematic diagram of repeated VNS (rVNS) procedures (right). Rats were administrated with rVNS for 6 d and subsequently subjected to behavioral tests. **(B)** Representative heatmaps showing activity (blue = low activity, red = high activity) in the OFT from sham and rVNS groups. **(C–E)** Anxiolytic action of rVNS in the OFT, including increased center crossings **(C)**, duration **(D)**, and distance **(E)** in the OFT. n = 10 rats for each group. **(F)** Representative heatmaps showing activity (blue = low activity, red = high activity) in the EPM from sham and rVNS groups. **(G–I)** Anxiolytic action of rVNS in the EPM, including increased the number of entries **(G)**, duration **(H)**, and distance **(I)** in the open arms. n = 9 rats for each group. **(J, K)** The latency to feed was decreased in the NSFT induced by rVNS **(J)**, but not affected food consumption **(K)**. n = 11 rats for sham, n = 13 rats for rVNS. Data are expressed as the mean ± SEM. *$p < 0.05$ and **$p < 0.01$; n.s., not significant. (For interpretation of the references to colour in this figure legend, the reader is referred to the Web version of this article.)

3. Results

3.1. Repeated VNS induces anxiolytic-like behaviors in male rats

Although growing evidence has identified that rVNS treatment with different parameters exhibits an anxiolytic effect in the behavioral tests (Furmaga et al., 2011; Noble et al., 2019; Shah et al., 2016), it is critical to identify optimal stimulation parameters involved in the anxiolytic effect of rVNS treatment. As shown in Fig. 1A, OFT, EPM and NSFT were used to estimate the anxiety levels of rats after 0 mA, 0.25 mA, 0.5 mA, and 0.75 mA current of rVNS treatment for 6 days. We found that rVNS treatment exhibited a dose response-dependent behavioral effect, and the anxiolytic effect started with current of 0.5 mA (Figs. S1A–H). By using the specific stimulation parameters (0.5 mA current, 500 μs pulse width at 30 Hz, stimulation cycle of 30 s on and 5 min off), it was found that rVNS significantly produced an anxiolytic effect, including increased exploration in the center of the open field (Fig. 1B). Such increased central exploration was evident in terms of both central crossing (sham: 5.300 ± 0.668, rVNS: 9.800 ± 1.245, n = 10, $p < 0.01$; Fig. 1C), central duration (sham: 12.230 ± 2.378 s, rVNS: 22.690 ± 3.551 s, n = 10, $p < 0.05$; Fig. 1D), and central distance (sham: 0.823 ± 0.180 m, rVNS: 1.922 ± 0.342 m, n = 10, $p < 0.05$; Fig. 1E). The increase in central exploration was not due to an increase in locomotor activity (Fig. S1D). A similar anxiolytic effect of rVNS was observed in

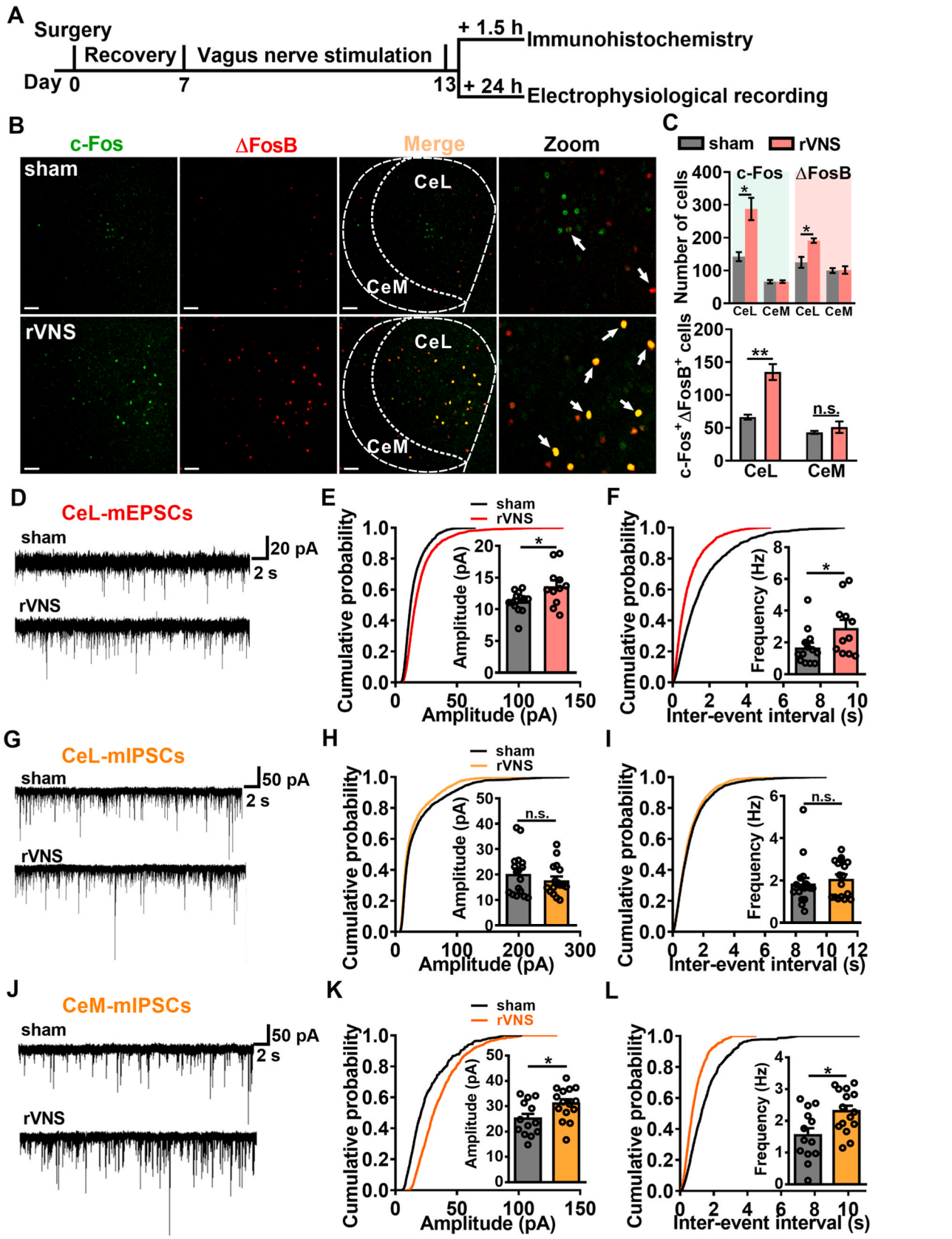

(caption on next page)

Fig. 2. rVNS increases excitatory neurotransmission in CeL and inhibitory neurotransmission in CeM. **(A)** The timeline of the experiments. **(B)** Expression of c-Fos positive cells (green) and ΔFosB positive cells (red) in the centrolateral amygdala (CeL) and centromedial amygdala (CeM) of rVNS-treated rats compared with sham rats. Arrows indicated co-labeled cells. Scale bar, 50 μm. **(C)** rVNS treatment increased c-Fos and ΔFosB expression in the CeL, but no difference in CeM. n = 12 slices from 3 rats per group. **(D)** Representative traces of AMPAR-mediated mEPSCs in the CeL from sham and rVNS-treated rats. Scale bar, 20 pA and 2 s. **(E)** Cumulative probabilities of mEPSCs amplitude and statistics of mEPSCs amplitude for representative cells from each group. rVNS increased the amplitude of mEPSCs by ~20% relative to sham-treated rat. n = 13 cells for sham, n = 11 cells for rVNS. **(F)** Cumulative probabilities of mEPSCs frequency and statistics of mEPSCs frequency for representative cells from each group. The frequency of mEPSCs was significantly increased in rVNS-treated rat. n = 13 cells for sham, n = 11 cells for rVNS. **(G)** Representative mIPSCs recording in the CeL neurons from sham and rVNS-treated rats. Scale bar, 50 pA and 2 s. **(H)** Cumulative probabilities of mIPSCs amplitude and statistics of mIPSCs amplitude for representative cells from each group. rVNS had no effect on the amplitude of mIPSCs in rVNS-treated rats. n = 17 cells for each group. **(I)** Cumulative probabilities of mIPSCs frequency and statistics of mIPSCs frequency for representative cells from each group. The frequency of mIPSCs was unaltered in rVNS-treated rats. n = 17 cells for each group. **(J)** Representative mIPSCs traces in CeM neurons from sham and rVNS group. Scale bars, 50 pA and 2 s. **(K)** Cumulative probabilities of mIPSCs amplitude and statistics of mIPSCs amplitude for representative cells from each group. The amplitude of mIPSCs recorded in CeM neuron was increased significantly in rVNS-treated rats. n = 13 cells for sham, n = 15 cells for rVNS. **(L)** Cumulative probabilities of mIPSCs frequency and statistics of mIPSCs frequency for representative cells from each group. rVNS significantly increased the frequency of mIPSCs. n = 13 cells for sham, n = 15 cells for rVNS. Data are expressed as the mean ± SEM. *p < 0.05, **p < 0.01; n.s., not significant. (For interpretation of the references to colour in this figure legend, the reader is referred to the Web version of this article.)

the EPM (Fig. 1F). Compared with the sham group, the entries (sham: 10.890 ± 1.409, rVNS: 15.560 ± 0.886, n = 9, p < 0.05; Fig. 1G), duration (sham: 72.080 ± 10.440 s, rVNS: 102.100 ± 4.527 s, n = 9, p < 0.05; Fig. 1H), and distance in the open arm (sham: 2.542 ± 0.390 m, rVNS: 4.398 ± 0.382 m, n = 9, p < 0.01; Fig. 1I) were increased in rVNS-treated rats. Furthermore, in the NSFT, the latency to feed was markedly reduced in rVNS-treated rats (sham: 248.900 ± 10.420 s, rVNS: 159.900 ± 23.830 s, n = 11–13, p < 0.01; Fig. 1J), but with no change in food consumption (Fig. 1K). Different from the anxiolytic phenotype, rVNS treatment did not induce an antidepressant effect in SPT (Figs. S1I and J) and FST (Fig. S1K), which was consistent with the previous reports (Furmaga et al., 2011). Taken together, the above results strongly suggest that rVNS administration produces anxiolytic-like behaviors in male rats.

3.2. rVNS increases excitatory synaptic transmission in CeL and inhibitory neurotransmission in CeM

The evidence from functional magnetic resonance imaging in clinic has demonstrated that rVNS increases the blood oxygenation-dependent activity in the amygdala (Bohning et al., 2001; Lomarev et al., 2002), indicating that the elevated activity of amygdala is induced by rVNS. CeA is considered as the major output nuclei of the amygdaloid complex and is critical in anxiety-like behavior (Calhoon and Tye, 2015; Shackman and Fox, 2016). As shown in Fig. 2A, the effect of rVNS on the activity of CeA was measured by detection and analysis of c-Fos/ΔFosB expression, which was the marker of neuronal activity to acute and chronic stimuli at 90 min after rVNS treatment, respectively. The results showed that compared with sham group, the numbers of c-Fos positive cells and ΔFosB positive cells, as well as c-Fos positive neurons that colocalized with ΔFosB, were significantly increased in the CeL of rVNS-treated rats, but no difference in CeM (Fig. 2B and C), suggesting that rVNS induces short-term and long-term changes in the excitability of CeL.

Vagal afferent neuronal cell bodies have central projections which terminate in NTS, and accumulating evidence suggests that NTS sends directly or indirectly noradrenergic signaling to CeA (Berthoud and Neuhuber, 2000). We found that rVNS increased the activity of the whole NTS (Figs. S2A–C), which was consistent with previous study (Cunningham et al., 2008). In order to ascertain the impact of rVNS on excitatory neurotransmission in CeL, the whole-cell patch-clamp recording was used to measure mEPSCs in CeL neurons. It was shown that the average amplitude of mEPSCs in CeL neurons was significantly increased from 11.210 ± 0.468 pA to 13.650 ± 0.929 pA, and the frequency of mEPSCs was elevated from 1.682 ± 0.309 Hz to 2.909 ± 0.513 Hz in rVNS-treated rats than that of sham-treated rats (Fig. 2D–F). However, the amplitude or frequency of mIPSCs in CeL neurons was no significant difference between sham and rVNS groups (Fig. 2G–I).

The primary output region of the CeA is the CeM, which mediates autonomic and behavioral responses associated with anxiety (Etkin et al., 2009; Krettek and Price, 1978b). In view of the activation of CeL GABAergic neurons drives inhibition of the CeM (Duvarci and Pare, 2014; Wahis et al., 2021), we further examined whether the inhibitory synaptic transmission of CeM was affected by rVNS. Electrophysiological results showed that the amplitude and frequency of mIPSCs were significantly increased in rVNS-treated rats (Fig. 2J-L), indicating that rVNS enhanced activity of CeL and increased the GABAergic transmission in CeM.

3.3. rVNS increases AMPAR trafficking in the CeL

Considering that rVNS enhances the glutamatergic neurotransmission via both presynaptic and postsynaptic mechanisms, we then detected whether rVNS treatment affected the surface expression of AMPARs in CeL. Western blotting analysis showed that the surface expression of GluA1 was elevated to 1.687 ± 0.194 of control induced by rVNS compared with sham group, without effect on total expression of GluA1 (Fig. 3A–C). However, the surface level and total amount of GluA2 (Figs. S3A–C) and N-methyl-D-aspartate-receptor (NMDAR) were unaltered in all groups (Figs. S3D–I).

We further administrated AMPAR antagonist CNQX to investigate the role of AMPAR in anxiolytic-like behaviors of rVNS. Rats were received bilaterally infusions of CNQX or vehicle in CeL, and subsequently treated with rVNS (Fig. 3D). The behavioral results showed that the central exploration in the OFT, including crossings, duration, and distance, was significantly reduced in rVNS + CNQX group compared with the rVNS + vehicle group (Fig. 3E–H). Correspondingly, CNQX prevented rVNS-induced anxiolytic effect compared with vehicle group, including fewer open arm entries, shorter open arm duration, and reduced open arm distance in the EPM (Fig. 3J-M). However, these manipulations did not influence the locomotor activity in the behavioral tests (Fig. 3I, N). Thus, the above results indicate that rVNS increases the glutamatergic synaptic neurotransmission and surface expression of GluA1 in CeL.

3.4. The anxiolytic-like behaviors induced by rVNS is independent of the vagal efferents

The vagus is a mixed nerve and composed of approximately 80% somatic afferents that communicated the state of the viscera to the brain (Ruffoli et al., 2011). Conventionally, the abdominal branch of the vagus nerve has been recognized as the core of the gut-brain axis (Han et al., 2018). We next investigated whether the anxiolytic effect of rVNS was primarily associated with the brain rather than periphery. To address this question, the subdiaphragmatic vagotomy (SDV) was performed to assess whether rVNS-induced anxiolytic-like behaviors were mediated by efferent vagal branches (Fig. 4A). In this experiment, all rats were operated by implantation of vagal nerve stimulators and sham surgery

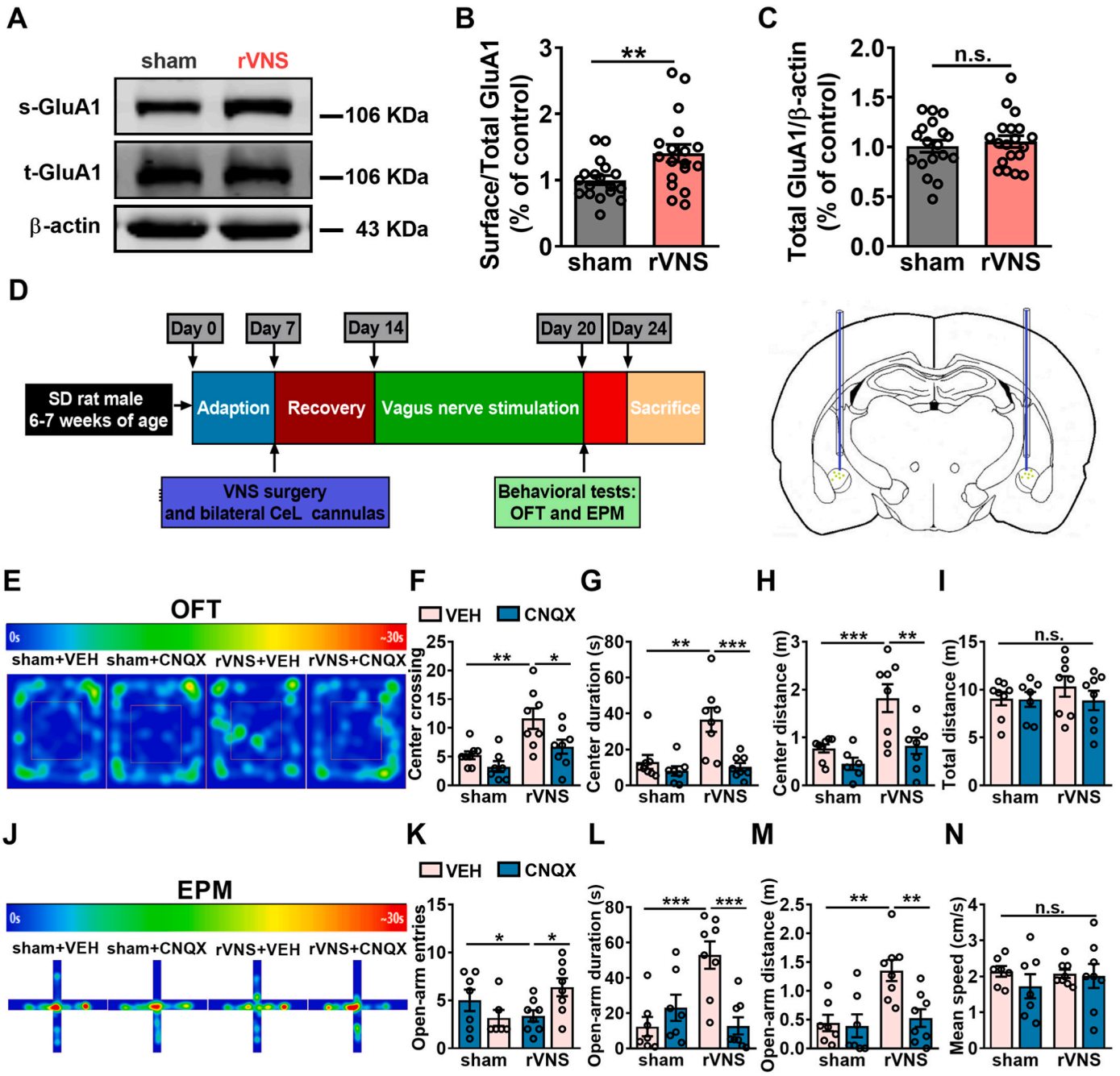

Fig. 3. rVNS increases AMPAR trafficking in CeL. **(A–C)** Western blotting results showing rVNS increased the ratio of surface protein/total protein (s/t)-GluA1, but not total GluA1 expression in the CeL. n = 18 for sham, n = 18–19 for rVNS. **(D)** Timeline of the experimental procedure (left). The rats that subjected to VNS surgery were implanted bilaterally with cannulas into CeL. Schematic of injection (right). After recovering for one week, rats were daily microinjected CNQX (20 μM) or vehicle (VEH) into CeL through cannulas 30 min before the rVNS program. **(E)** The representative heatmaps showing activity (blue = low activity, red = high activity) in the OFT from sham + VEH, sham + CNQX, rVNS + VEH, and rVNS + CNQX groups. **(F–I)** CNQX prevented the increased central exploration including central crossing **(F)**, duration **(G)**, and distance **(H)** in the OFT induced by rVNS, while the locomotor activity was unaltered **(I)**. n = 6–8 rats for each group. **(J)** The representative heatmaps showing activity in the EPM from sham + VEH, sham + CNQX, rVNS + VEH, and rVNS + CNQX groups. **(K–N)** The open arm exploration including open arm entries **(K)**, duration **(L)**, and distance **(M)** were both reduced in the rVNS + CNQX groups than that of rVNS + VEH groups, while the mean speed was unaltered **(N)**. n = 6–8 rats for each group. Data are expressed as the mean ± SEM. *p < 0.05, **p < 0.01, ***p < 0.001; n.s., not significant. (For interpretation of the references to colour in this figure legend, the reader is referred to the Web version of this article.)

or SDV (Fig. S4A). CCK-8 treatment significantly suppressed the food intake in the control rats, but not in the SDV-treated rats, which was consistent with the previous study (Davis et al., 2020) (Fig. S4B). The behavioral results showed that SDV failed to affect central crossings, central duration, and central distance in the OFT (Fig. 4B–E) and the open arm entries, duration, and distance in the EPM (Fig. 4F–I) induced by rVNS. In addition, the vagotomy did not influence the baseline anxiety of sham rats, and none of manipulation affected locomotor activity (Fig. 4J and K). SDV also did not influence the anxiolytic-like behavior in the NSFT induced by rVNS (Fig. 4L and M). Thus, the anxiolytic effect of rVNS is independent of the vagal efferents.

To elucidate whether the vagal afferent fibers mediate the anxiolytic

effect via regulating the activity of CeL neurons, we further measured AMPAR-medicated mEPSCs in CeL slices after SDV. It was found that the amplitude and frequency of AMPAR-mediated mEPSCs were significantly increased in the rVNS-treated rats compared with sham-treated rats, but with no difference between rVNS + SDV group and the rVNS + sham group (Fig. 4N–P). Thus, these results further provide the evidence that rVNS exerts an anxiolytic effect via facilitating the excitatory neurotransmission in CeL, which is independent of vagal efferents.

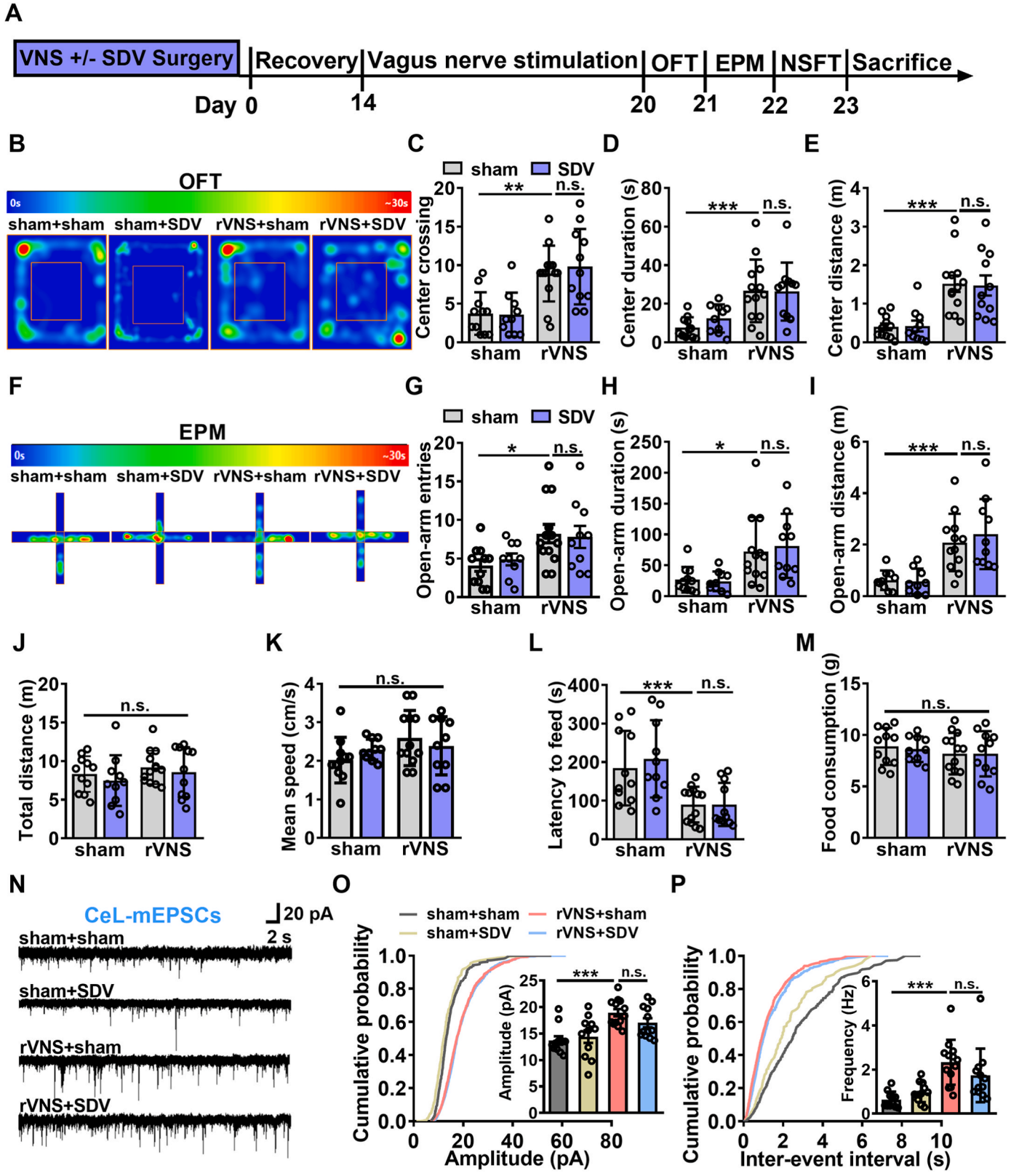

(caption on next page)

Fig. 4. The anxiolytic-like behaviors induced by rVNS is independent of the vagal efferents. **(A)** The experimental procedure. **(B)** The representative heatmaps showing activity (blue = low activity, red = high activity) in the OFT from sham + sham, sham + SDV, rVNS + sham, and rVNS + SDV groups. **(C–E)** SDV did not affect the effect of rVNS on the number of central entries **(C)**, duration **(D)** and distance **(E)** in the OFT. n = 10–13 rats for each group. **(F)** The representative heatmaps showing activity in the EPM from sham + sham, sham + SDV, rVNS + sham, and rVNS + SDV groups. **(G–I)** SDV did not affect the effect of rVNS on the entries **(G)**, duration **(H)**, and distance **(I)** in the open arms. n = 9–13 rats for each group. **(J, K)** SDV treatment did not affect the locomotor activity. **(L, M)** SDV failed to block the reduced latency to feed in NSFT induced by rVNS **(L)**, and the total food consumption were not affected **(M)**. n = 10–13 rats for each group. **(N)** Representative traces of mEPSCs in the CeL from sham + sham, sham + SDV, rVNS + sham, and rVNS + SDV groups. Scale bar, 20 pA and 2 s. **(O)** Cumulative probabilities and average amplitudes of mEPSCs in the CeL from the sham + sham, sham + SDV, rVNS + sham, and rVNS + SDV groups. SDV failed to block the increased amplitude of mEPSCs induced by rVNS. n = 11 cells for sham + sham, n = 11 cells for sham + SDV, n = 13 cells for rVNS + sham, n = 12 cells for rVNS + SDV. **(P)** Cumulative probabilities and frequency of mEPSCs in the CeL from the sham + sham, sham + SDV, rVNS + sham, and rVNS + SDV groups. Compared with sham groups, the frequency of mEPSCs were both increased in rVNS groups, while SDV treatment did not abolish the effect of rVNS. n = 11 cells for sham + sham, n = 11 cells for sham + SDV, n = 13 cells for rVNS + sham, n = 12 cells for rVNS + SDV. Data are expressed as the mean ± SEM. *p < 0.05, **p < 0.01, ***p < 0.001; n.s., not significant. (For interpretation of the references to colour in this figure legend, the reader is referred to the Web version of this article.)

3.5. Chemogenetic inhibition of CeL neurons abolishes anxiolytic effect in male rats induced by rVNS

Considering that rVNS increased c-Fos positive cells in the CeL, we specifically manipulated the activity of CeL neurons through chemogenetics to determine whether the increased activity of CeL neurons was involved in the anxiolytic effect induced by rVNS. The h4MD(Gi), a CNO-based inhibitory DREADD (Urban and Roth, 2015) was expressed through the adeno-associated viruses (AAV-hSyn-Cre and AAV-Ef1α-DIO-hM4D(Gi)-mCherry) in CeL (Fig. 5A). Four weeks later, the abundant expression of hM4D(Gi) in CeL neurons was verified by mCherry expression (Fig. 5B). Then, we performed whole-cell patch--clamp recording to validate the efficacy of chemogenetic inhibition. We found that bath application with the synthetic hM4D(Gi) ligand CNO (5 μM) significantly suppressed the firing of APs in CeL neurons, indicating that CNO effectively inhibits the neuronal activity of CeL (Fig. 5C and D).

We then investigated the impact of chemogenetic inhibition of CeL activity in rVNS-induced anxiolytic effect. CNO (5 mg/kg) or vehicle was intraperitoneally injected 30 min before VNS, and the process was performed for a continuous six-day. Behavioral tests showed that chemogenetic inhibition of CeL neurons caused a significant decrease in central crossing, central duration, and central distance relative to the rVNS-treated rats in the OFT (Fig. 5E–H). The entries, duration, and distance in the open-arm were also reduced in the EPM (Fig. 5I-L). Furthermore, the latency to feed in NSFT was longer in rVNS + CNO group (285.600 ± 28.010 s) than that of rVNS group (124.800 ± 28.080 s) (Fig. 5M). However, the hM4D(Gi) manipulation had no effect on baseline anxiety of sham rats, and none of manipulation affected locomotor activity (Fig. 5N). In addition, considering that CNO was converted to clozapine (CLZ) and CLZ might be effective for anxiety (Gomez et al., 2017), the effect of CNO on control rats was investigated. It was found that CNO application did not affect the baseline anxiety of control rats (Fig. S5). Thus, inhibition of CeL neurons abolishs the anxiolytic effect induced by rVNS.

To determine whether chemogenetic inhibition of the CeL neurons inhibited glutamatergic synaptic transmission, the surface expression of GluA1 was quantified. It was shown that CNO blocked the increased surface expression of GluA1 from 1.563 ± 0.119 to 0.729 ± 0.078 of control induced by rVNS (Fig. 5O and P), whereas the total protein levels remained unchanged (Fig. 5Q). Additionally, we further measured mIPSCs in CeM slices after chemogenetic inhibition of CeL neurons. Correspondingly, whole-cell patch-clamp recording showed that application with CNO abolished the increased amplitude and frequency of mIPSCs in CeM of rVNS groups, indicating that inhibiting activity of CeL neurons abolishes the increased mIPSCs in CeM induced by rVNS (Fig. 5R–T). Taken together, these indicate that chemogenetic inhibition of CeL neurons undermines the anxiolytic activity and the AMPARs trafficking induced by rVNS.

3.6. Pharmacological inhibition of β-ARs in CeL abolishes rVNS-induced anxiolytic effect

Therefore, we further examined whether exogenous NE could mimic rVNS-induced increase in AMPAR-mediated mEPSCs *in vitro*. The results showed that bath application with β-ARs agonist isoproterenol (ISO) in CeL increased the amplitude of mEPSCs (Figs. S6A and B), but the frequency of mEPSCs was only slightly increased (Fig. S6C). Moreover, β-ARs antagonist propranolol, but not α-adrenergic receptor antagonist phentolamine, reduced the amplitude of mEPSCs relative to control, while the frequency of mEPSCs were unaltered in all groups (Fig. 6A–C & Figs. S6D–F). These results suggest that noradrenergic system enhances glutamatergic neurotransmission in the CeL through activation of β-ARs.

To clarify the role of β-ARs in anxiolytic effect of rVNS, rats were received bilaterally intra-CeL infusions of propranolol or vehicle, and subsequently treated with rVNS. The behavioral results showed that propranolol prevented rVNS-induced anxiolytic effect compared with vehicle group, including fewer central crossings, shorter central duration, and reduced central distance in the OFT (Fig. 6D–G), as well as decreased open arm exploration in the EPM (Fig. 6H–K) and the longer latency to feed in the NSFT (Fig. 6L). However, propranolol had no effect on baseline anxiety, and none of the manipulations affected locomotor activity in the sham-treated rats (Fig. 6M). Next, we further investigate whether the inhibition of β-ARs could prevent the increased AMPAR trafficking induced by rVNS, and found that propranolol also reduced surface expression of GluA1 from 1.388 ± 0.095 to 0.844 ± 0.131 of control induced by rVNS, but the total GluA1 protein was unchanged (Fig. 6N–P). This is consistent with the electrophysiological results *in vitro*. Together, β-ARs contribute to an increase in AMPAR activity in the CeL of rats that are exposed to rVNS, at least partially, the synaptic delivery of GluA1-containing AMPAR may be responsible for this process.

4. Discussion

In the present study, we provide direct evidence that rVNS promotes AMPAR function on CeL neurons by activation of noradrenergic signaling, and then enhances inhibitory transmission of CeM output neurons, resulting in anxiolysis. We showed that rVNS-mediated noradrenergic system in CeL was critical for the surface stability of AMPAR and AMPAR-mediated mEPSCs, contributing to rVNS-induced anxiolytic effect. Moreover, chemogenetic inhibition of the CeL neurons attenuated inhibitory inputs into CeM output neurons and then abolished rVNS-induced anxiolytic effect.

Several studies have reported that both acute and chronic VNS treatment produces an anxiolytic effect in rats, as is shown in EPM and NSFT (Furmaga et al., 2011; Mathew et al., 2020; Noble et al., 2019). In our study, we found that repeated, but not single, VNS treatment exhibited anxiolytic-like behaviors. In addition, depression-like behaviors were unchanged, resulting from the need for a more persistent treatment following this stimulation program, which is consistent with

the previous study (Furmaga et al., 2011). As discussed above, different stimulation programs produce a distinct therapeutic effect for anxiety-like behaviors (Biggio et al., 2009; Furmaga et al., 2011; Mathew et al., 2020; Noble et al., 2019), indicating that establishing a uniform and rational VNS protocol for anxiety research is imperative. Our stimulation program displayed a consistent anxiolytic-like effect in various behavioral tests, including OFT, EPM and NSFT. Previous studies have shown that rVNS facilitates the metabolic activity in amygdala. It has been identified that the activity of CeL neurons is positively correlated to anxiolytic effect of benzodiazepines (Griessner

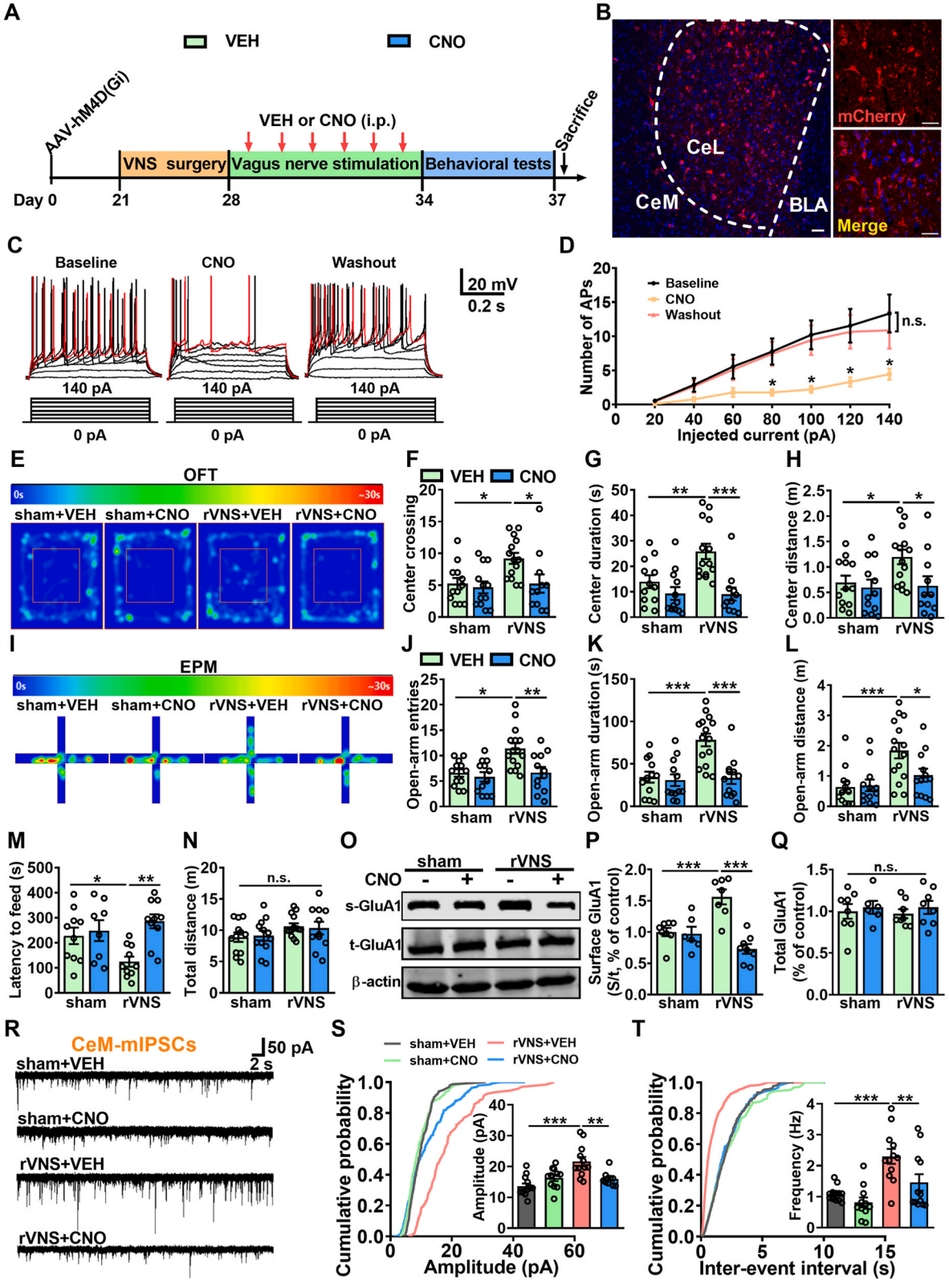

(caption on next page)

Fig. 5. Chemogenetic inhibition of CeL neurons abolishes anxiolytic effect in male rats induced by rVNS. **(A)** Experimental timeline and schematic representation of the viral injection of hM4D(Gi)-DREADD (designer receptor exclusively activated by designer drugs) for behavioral experiments in male rats. An adeno-associated virus (AAV) cocktail, fluorescently tagged with mCherry (300 nl per side), was injected bilaterally into CeL 3 weeks before VNS surgery. Clozapine-N-oxide (CNO) (5 mg/kg, i.p.) or vehicle (VEH) was administered 30 min before rVNS. **(B)** The confocal images of representative fields showing mCherry and DAPI expression in CeL. Scale bar, 30 μm. **(C)** Representative traces of action potential in CeL neurons before, during and after CNO (5 μM) perfusion. **(D)** Number of APs in CeL neurons was decreased by current injections at 80 pA–140 pA. n = 9 cells for each group. **(E)** The representative heatmaps showing activity in the OFT from sham + VEH, sham + CNO, rVNS + VEH, and rVNS + CNO groups. **(F–H)** CNO abolished anxiolytic-like behaviors induced by rVNS, including the number of entries **(F)**, the duration **(G)**, and the distance **(H)** in the central zone. n = 11–14 rats for each group. **(I)** The representative heatmaps showing activity in the EPM from sham + VEH, sham + CNO, rVNS + VEH, and rVNS + CNO groups. **(J–L)** CNO prevented anxiolytic-like behaviors by rVNS, including the number of entries **(J)**, duration **(K)**, and the distance **(L)** in the open arms. n = 12–15 rats for each group. **(M)** rVNS + CNO-treated rats displayed the increased latency to feed in the NSFT compared with rVNS + VEH-treated rats. n = 10 rats for sham + VEH, n = 8 rats for sham + CNO, n = 10 rats for rVNS + VEH, and n = 10 rats for rVNS + CNO. **(N)** CNO treatment did not affect the locomotor activity. **(O–Q)** Western blotting results showing administration of CNO prevented the increase in the ratio of surface/total GluA1 protein (s/t) induced by rVNS, and there was no difference of the total GluA1 expression in CeL. n = 6–8 for each group. **(R)** Representative mIPSCs traces in CeM neurons from sham + VEH, sham + CNO, rVNS + VEH, and rVNS + CNO group. Scale bars, 50 pA and 2 s. **(S)** Cumulative probabilities of mIPSCs amplitude and statistics of mIPSCs amplitude for representative cells from each group. The increased amplitude of mIPSCs recorded in CeM neuron in rVNS-treated rats was reversed by CNO. n = 11–12 cells for each group. **(T)** Cumulative probabilities of mIPSCs frequency and statistics of mIPSCs frequency for representative cells from each group. CNO significantly decreased the increased frequency of mIPSCs in rVNS-treated rats. Data are expressed as the mean ± SEM. *p < 0.05, **p < 0.01, ***p < 0.001; n.s., not significant.

et al., 2018; Thompson and Rosen, 2006). Our findings showed that rVNS improved anxiolytic-like behaviors, accompanied with the increased neuronal activity in CeL. Previous study reports that chemogenetic activation of enkephalinergic neurons, a subpopulation of neurons in CeL that overlapped with protein kinase Cδ (PKCδ) expressing neurons (Haubensak et al., 2010; Poulin et al., 2008), is sufficient to cause anxiolysis (Paretkar and Dimitrov, 2019). Moreover, we found that chemogenetic inhibition of the CeL neurons reversed rVNS-mediated anxiolytic effect. Interestingly, SDV treatment precluded the role of vagal efferent in glutamatergic neurotransmission in CeL and anxiolytic effect induced by VNS, while SDV itself did not manipulate anxiety-like behaviors. The previous report showed that subdiaphragmatic vagal deafferentation reduces anxiety-like behavior (Klarer et al., 2014), which can be explained by the different surgical content. Therefore, our results provide the first direct evidence that the potentiation of CeL activity is responsible for rVNS-induced anxiolytic-like behaviors. However, whether the anxiolytic effect of rVNS on female rats needs further investigation in the future.

NTS is the main brainstem area of integration for vagal afferents, and then directly provides noradrenergic signaling to CeA (Berthoud and Neuhuber, 2000; Chen et al., 2019). Chen et al. shows that NTS neurons can negatively regulate anxiety-like behavior (Chen et al., 2019). LC, which receives innervation from NTS (Van Bockstaele, Peoples and Telegan, 1999), is the major NE brainstem nucleus that sends projections to many brain areas, including CeA (Campese et al., 2017; Gu et al., 2020). Considering that rVNS increased the firing rate of LC noradrenergic neurons (Dorr and Debonnel, 2006), we speculate that NTS or LC may be the potential resource of NE in CeA. Previous studies demonstrate that rVNS increases the extracellular NE level and then facilitates noradrenergic system-mediated neuroplasticity (Alexander et al., 2017; Biggio et al., 2009). β-ARs activation enhances glutamatergic transmission in CeL, via increasing presynaptic co-release of NE and glutamate (Silberman and Winder, 2013), and our results showed that rVNS increased the frequency of mEPSCs in CeL, suggesting that rVNS might elevate NE levels that led to an increased neuronal activation in CeL. Importantly, the activation of β-ARs by NE is thought to mediate memory process, defensive behavior, and anxiety-like behavior (Liang et al., 1986; Watanabe et al., 2003; Zhu et al., 2017). There are several findings indicate that activation of the noradrenergic system decreases anxiety-like behavior and promotes an active coping strategy in response to stressors (Chen et al., 2019; Khoshbouei et al., 2002), which is crucial for the behavioral effects of rVNS. We found that microinjection of propranolol into CeL abolished the anxiolytic-like behaviors induced by rVNS. Our findings indicate that rVNS treatment produces anxiolytic effect, at least partially, β-ARs might be responsible for this process.

There is several evidence that alteration of neuronal activity is a form of neuroplasticity (Samson and Pare, 2005) and synaptic recruitment of AMPARs plays a crucial role in activity-dependent synaptic plasticity (Zhou et al., 2019). AMPARs are ionotropic glutamate receptors that mediate majority of the fast-excitatory neurotransmission in the brain. Tye et al. found that intra-CeL infusion of AMPAR antagonist abolished light-induced reduction in anxiety (Tye et al., 2011). Similarly, we observed that AMPAR antagonist CNQX abolished rVNS-induced anxiolytic-like behaviors. Hu et al. found that NE facilitated the trafficking of GluA1-containing AMPARs (Hu et al., 2007). Activation of β-ARs by NE stimulates the intracellular cAMP-PKA signaling, contributing to the excitatory synaptic transmission in the lateral amygdala (Patriarchi et al., 2018). Based on these insights, we can assume that GluA1-containing AMPAR function in CeL is momentous to the anxiolytic-like behaviors induced by rVNS. We found that treatment with rVNS promoted GluA1-containing AMPAR function in CeL, which is abolished by microinjection of CNQX into CeL. Furthermore, the increased AMPAR-mediated mEPSCs induced by rVNS could be mimicked by β-ARs agonist ISO and abolished by β-ARs antagonist propranolol. Most importantly, pharmacologic inhibition of β-ARs in CeL undermined the increased surface expression of GluA1 and the anxiolytic-like behaviors induced by rVNS. Therefore, the noradrenergic system in CeL contributed to the effect of AMPAR trafficking and anxiolytic-like behaviors.

However, several reports have shown that the activity of CeA neurons is positively correlated with negative emotional behaviors (Kalin et al., 2004; Ventura-Silva et al., 2013). This discrepancy may be due to the complex inscape of CeA microcircuitry, which makes it difficult to interpret many electrophysiological and behavioral tests. CeA microcircuitry has been the focus in the past few years (Ciocchi et al., 2010; Griessner et al., 2018; Tye et al., 2011). CeM, the primary output region of CeA, receives inhibitory inputs from CeL GABAergic neurons (Duvarci and Pare, 2014; Janak and Tye, 2015; Krettek and Price, 1978a; Tye et al., 2011), suggesting that both activation of CeL and inactivation of CeM can induce anxiolysis. Consistent with these studies, we observed that the amplitude and frequency of mIPSCs were significantly increased in the CeM induced by rVNS. Furthermore, chemogenetic inhibition of CeL neurons abolished the enhanced inhibitory transmission in CeM induced by rVNS. Our results provide evidence that rVNS-induced excitation of CeL neurons promotes inhibitory transmission of CeM output neurons and leads to anxiolysis. The findings presented here indicate that activation of β-ARs might enhance glutamatergic neurotransmission in CeL. Ultimately, β-ARs-mediated the enhancement of CeL excitation would be predicted to increase inhibitory transmission of CeM neurons and in turn relieve anxiety-like behaviors. CeL consists of two non-overlapping populations of GABAergic neurons, which can be distinguished by their expression markers PKCδ and somatostatin (SOM) (Li et al., 2013). $PKC\delta^{+}$ neurons are tightly regulated by local inhibitory

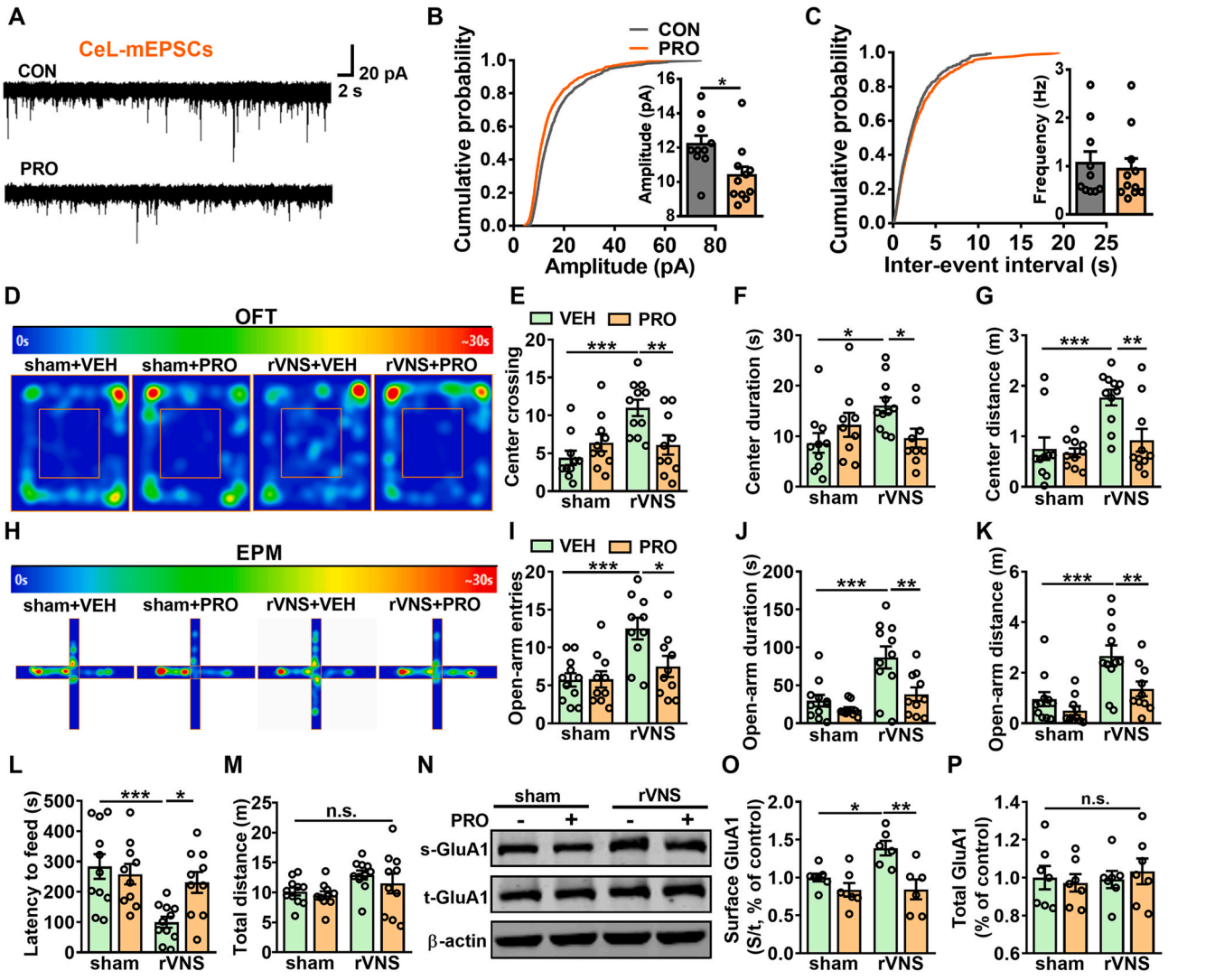

Fig. 6. Pharmacological inhibition of β-ARs in CeL abolishes rVNS-induced anxiolytic effect. **(A)** Representative mEPSCs traces in CeL from β-ARs antagonist propranolol (PRO) incubation. **(B)** Cumulative probabilities of mEPSCs amplitude and statistics of mEPSCs amplitude for representative cells from each group. The amplitude of mEPSCs after propranolol incubation was significantly decreased. n = 10 cells for CON, n = 11 cells for PRO. **(C)** Cumulative probabilities of mEPSCs frequency and statistics of mEPSCs frequency for representative cells from each group. Propranolol did not affect the frequency of mEPSCs. n = 10 cells for CON, n = 11 cells for PRO. **(D)** The representative heatmaps showing activity in the OFT from sham + VEH, sham + PRO, rVNS + VEH, and rVNS + PRO groups. **(E–G)** Propranolol abolished anxiolytic-like behaviors induced by rVNS, including reduced the number of entries **(E)**, duration **(F)**, and distance **(G)** in the central zone. n = 9–11 rats for each group. **(H)** The representative heatmaps showing activity in the EPM from sham + VEH, sham + PRO, rVNS + VEH, and rVNS + PRO groups. **(I–K)** rVNS + PRO group significantly decreased the number of entries **(I)**, duration **(J)**, and distance **(K)** in the open arms compared with rVNS + VEH group. n = 10–11 rats for each group. **(L)** Propranolol deteriorated the latency to feed in the NSFT of rVNS-treated rats. n = 10–11 rats for reach group. **(M)** Propranolol treatment did not affect the locomotor activity. **(N–P)** Western blotting results showed the effects of β-ARs antagonist propranolol in CeL before rVNS treatment on membrane insertion of GluA1. rVNS increased the ratio of surface protein/total protein (s/t)-GluA1, while administration of propranolol restrained the increased ratio of surface protein/total protein (s/t)-GluA1 from rVNS. There was no difference of the total GluA1 expression in CeL. n = 6–7 for each group. Data are expressed as the mean ± SEM. *p < 0.05, **p < 0.01, ***p < 0.001; n.s., not significant.

connection with SOM$^+$ neurons and project to the CeM. Inhibition of PKCδ$^+$ neurons was associated with disinhibition of CeM output neurons (Haubensak et al., 2010). Additionally, recent study has identified that PKCδ$^+$ neurons in CeL are necessary and sufficient to induce the diazepam anxiolytic effect, which is indicative of an anxiolytic effect of PKCδ$^+$ neurons (Griessner et al., 2018). Accordingly, future study is needed to further explore its intrinsic mechanism of cell-type specific neural circuits about rVNS anxiolytic effect.

In conclusion, the present study uncovers a crucial mechanism for rVNS in anxiolytic effect. Our study couples the modulation of AMPAR trafficking and synaptic plasticity in CeL with anxiolytic-like behaviors induced by rVNS via the noradrenergic system in CeL. Moreover, rVNS-driven excitation of CeL neurons enhances inhibitory transmission of CeM output neurons. Taken together, these results suggest that rVNS is critical for anxiolytic-like behaviors, and highlights rVNS as a potential novel therapeutic strategy for the treatment of anxiety disorders.

CRediT authorship contribution statement

Shao-Qi Zhang: Methodology, Investigation, Formal analysis, Data curation, performed western blotting, behavioral tests, immunofluorescence and analyzed the data, Writing – original draft, The paper was written. **Zhi-Xuan Xia:** performed behavioral tests and electrophysiology recording. **Qiao Deng:** performed the electrophysiology recording. **Ping-Fen Yang:** performed stereotaxic surgery. **Li-Hong Long:** provided technical support, Resources, The paper was written.

Fang Wang: Conceptualization, Writing – review & editing, Project administration, Supervision, Funding acquisition, All studies were conceptualized and designed, Writing – original draft, The paper was written. **Jian-Guo Chen:** Conceptualization, All studies were conceptualized and designed, Writing – review & editing, Project administration, Supervision, Funding acquisition, The paper was written.

Declaration of competing interest

The authors declare no competing interests.

Acknowledgments

This work was supported by the Foundation for National Key R&D Program of China (Grant No. 2021ZD0202900 to J-GC), National Natural Science Foundation of China (Grant Nos. 82130110 to J-GC, U21A20363 to FW and 81573414 to L-HL), Innovative Research Groups of National Natural Science Foundation of China (Grant No. 81721005 to JGC and FW), Program for Changjiang Scholars and Innovative Research Team in University (Grant No. IRT13016 to J-GC).

Appendix A. Supplementary data

Supplementary data to this article can be found online at https://doi.org/10.1016/j.ynstr.2022.100453.

References

Alexander, G.M., Huang, Y.Z., Soderblom, E.J., He, X.P., Moseley, M.A., McNamara, J.O., 2017. Vagal nerve stimulation modifies neuronal activity and the proteome of excitatory synapses of amygdala/piriform cortex. J. Neurochem. 140, 629–644. https://doi.org/10.1111/jnc.13931.

Beitchman, J.A., Griffiths, D.R., Hur, Y., Ogle, S.B., Bromberg, C.E., Morrison, H.W., et al., 2019. Experimental traumatic brain injury induces chronic glutamatergic dysfunction in amygdala circuitry known to regulate anxiety-like behavior. Front. Neurosci. 13, 1434. https://doi.org/10.3389/fnins.2019.01434.

Berthoud, H.R., Neuhuber, W.L., 2000. Functional and chemical anatomy of the afferent vagal system. Auton. Neurosci. 85, 1–17. https://doi.org/10.1016/S1566-0702(00)00215-0.

Biggio, F., Gorini, G., Utzeri, C., Olla, P., Marrosu, F., Mocchetti, I., et al., 2009. Chronic vagus nerve stimulation induces neuronal plasticity in the rat hippocampus. Int. J. Neuropsychopharmacol. 12, 1209–1221. https://doi.org/10.1017/S1461145709000200.

Bohning, D.E., Lomarev, M.P., Denslow, S., Nahas, Z., Shastri, A., George, M.S., 2001. Feasibility of vagus nerve stimulation-synchronized blood oxygenation level-dependent functional MRI. Invest. Radiol. 36, 470–479. https://doi.org/10.1097/00004424-200108000-00006.

Calhoon, G.G., Tye, K.M., 2015. Resolving the neural circuits of anxiety. Nat. Neurosci. 18, 1394–1404. https://doi.org/10.1038/nn.4101.

Campese, V.D., Soroeta, J.M., Vazey, E.M., Aston-Jones, G., LeDoux, J.E., Sears, R.M., 2017. Noradrenergic Regulation of Central Amygdala in Aversive Pavlovian-To-Instrumental Transfer. https://doi.org/10.1523/ENEURO.0224-17.2017 eNeuro. 4, ENEURO.0224-17.

Carmichael, R.E., Wilkinson, K.A., Craig, T.J., Ashby, M.C., Henley, J.M., 2018. MEF2A regulates mGluR-dependent AMPA receptor trafficking independently of Arc/Arg3.1. Sci. Rep. 8, 5263. https://doi.org/10.1038/s41598-018-23440-0.

Carvalho, M.C., Moreira, C.M., Zanoveli, J.M., Brandao, M.L., 2012. Central, but not basolateral, amygdala involvement in the anxiolytic-like effects of midazolam in rats in the elevated plus maze. J. Psychopharmacol. 26, 543–554. https://doi.org/10.1177/0269881110389209.

Chen, Y.W., Das, M., Oyarzabal, E.A., Cheng, Q., Plummer, N.W., Smith, K.G., et al., 2019. Genetic identification of a population of noradrenergic neurons implicated in attenuation of stress-related responses. Mol. Psychiatr. 24, 710–725. https://doi.org/10.1038/s41380-018-0245-8.

Ciocchi, S., Herry, C., Grenier, F., Wolff, S.B., Letzkus, J.J., Vlachos, I., et al., 2010. Encoding of conditioned fear in central amygdala inhibitory circuits. Nature 468, 277–282. https://doi.org/10.1038/nature09559.

Craske, M.G., Stein, M.B., 2016. Anxiety. Lancet 388, 3048–3059. https://doi.org/10.1016/S0140-6736(16)30381-6.

Cunningham, J.T., Mifflin, S.W., Gould, G.G., Frazer, A., 2008. Induction of c-Fos and DeltaFosB immunoreactivity in rat brain by Vagal nerve stimulation. Neuropsychopharmacology 33, 1884–1895. https://doi.org/10.1038/sj.npp.1301570.

Davis, E.A., et al., 2020. Ghrelin signaling affects feeding behavior, metabolism, and memory through the vagus nerve. Curr. Biol. 30, 4510–4518. https://doi.org/10.1016/j.cub.2020.08.069.

Dorr, A.E., Debonnel, G., 2006. Effect of vagus nerve stimulation on serotonergic and noradrenergic transmission. J. Pharmacol. Exp. Therapeut. 318, 890–898. https://doi.org/10.1124/jpet.106.104166.

Duvarci, S., Pare, D., 2014. Amygdala microcircuits controlling learned fear. Neuron 82, 966–980. https://doi.org/10.1016/j.neuron.2014.04.042.

Etkin, A., Prater, K.E., Schatzberg, A.F., Menon, V., Greicius, M.D., 2009. Disrupted amygdalar subregion functional connectivity and evidence of a compensatory network in generalized anxiety disorder. Arch. Gen. Psychiatr. 66, 1361–1372. https://doi.org/10.1001/archgenpsychiatry.2009.104.

Faber, E.S., Delaney, A.J., Power, J.M., Sedlak, P.L., Crane, J.W., Sah, P., 2008. Modulation of SK channel trafficking by beta adrenoceptors enhances excitatory synaptic transmission and plasticity in the amygdala. J. Neurosci. 28, 10803–10813. https://doi.org/10.1523/JNEUROSCI.1796-08.2008.

Fan, J., Li, D., Chen, H.S., Huang, J.G., Xu, J.F., Zhu, W.W., et al., 2019. Metformin produces anxiolytic-like effects in rats by facilitating GABAA receptor trafficking to membrane. Br. J. Pharmacol. 176, 297–316. https://doi.org/10.1111/bph.14519.

Furmaga, H., Shah, A., Frazer, A., 2011. Serotonergic and noradrenergic pathways are required for the anxiolytic-like and antidepressant-like behavioral effects of repeated vagal nerve stimulation in rats. Biol. Psychiatr. 70, 937–945. https://doi.org/10.1016/j.biopsych.2011.07.020.

George, M.S., Ward Jr., H.E., Ninan, P.T., Pollack, M., Nahas, Z., Anderson, B., et al., 2008. A pilot study of vagus nerve stimulation (VNS) for treatment-resistant anxiety disorders. Brain Stimul. 1, 112–121. https://doi.org/10.1016/j.brs.2008.02.001.

Gomez, J.L., Bonaventura, J., Lesniak, W., Mathews, B.W., Sysa-Shah, p., Rodriguez, A. L., et al., 2017. Chemogenetics revealed: DREADD occupancy and activation via converted clozapine. Science 357, 503–507. https://doi.org/10.1126/science.aan2475.

Griessner, J., Pasieka, M., Bohm, V., Grossl, F., Kaczanowska, J., Pliota, P., et al., 2018. Central amygdala circuit dynamics underlying the benzodiazepine anxiolytic effect. Mol. Psychiatr. 26, 534–544. https://doi.org/10.1038/s41380-018-0310-3.

Gu, Y., Piper, W.T., Branigan, L.A., Vazey, E.M., Aston-Jones, G., Lin, L., et al., 2020. A brainstem-central amygdala circuit underlies defensive responses to learned threats. Mol. Psychiatr. 25, 640–654. https://doi.org/10.1038/s41380-019-0599-6.

Han, W., Tellez, L.A., Perkins, M.H., Perez, I.O., Qu, T., Ferreira, J., et al., 2018. A neural circuit for gut-induced reward. Cell 175, 887–888. https://doi.org/10.1016/j.cell.2018.10.018.

Haubensak, W., Kunwar, P.S., Cai, H., Ciocchi, S., Wall, N.R., Ponnusamy, R., et al., 2010. Genetic dissection of an amygdala microcircuit that gates conditioned fear. Nature 468, 270–276. https://doi.org/10.1038/nature09553.

Hu, H., Real, E., Takamiya, K., Kang, M.G., Ledoux, J., Huganir, R.L., et al., 2007. Emotion enhances learning via norepinephrine regulation of AMPA-receptor trafficking. Cell 131, 160–173. https://doi.org/10.1016/j.cell.2007.09.017.

Janak, P.H., Tye, K.M., 2015. From circuits to behaviour in the amygdala. Nature 517, 284–292. https://doi.org/10.1038/nature14188.

Jia, H.G., Rao, Z.R., Shi, J.W., 1997. Evidence of gamma-aminobutyric acidergic control over the catecholaminergic projection from the medulla oblongata to the central nucleus of the amygdala. J. Comp. Neurol. 381, 262–281. https://doi.org/10.1002/(sici)1096-9861(19970512)381:3<262::aid-cne2>3.0.co;2–0.

Kalin, N.H., Shelton, S.E., Davidson, R.J., 2004. The role of the central nucleus of the amygdala in mediating fear and anxiety in the primate. J. Neurosci. 24, 5506–5515. https://doi.org/10.1523/JNEUROSCI.0292-04.2004.

Khoshbouei, H., Cecchi, M., Dove, S., Javors, M., Morilak, D.A., 2002. Behavioral reactivity to stress: amplification of stress-induced noradrenergic activation elicits a galanin-mediated anxiolytic effect in central amygdala. Pharmacol. Biochem. Behav. 71, 407–417. https://doi.org/10.1016/s0091-3057(01)00683-9.

Klarer, M., Arnold, M., Gunther, L., Winter, C., Langhans, W., Meyer, U., 2014. Gut vagal afferents differentially modulate innate anxiety and learned fear. J. Neurosci. 34, 7067–7076. https://doi.org/10.1523/JNEUROSCI.0252-14.2014.

Krettek, J.E., Price, J.L., 1978a. Amygdaloid projections to subcortical structures within the basal forebrain and brainstem in the rat and cat. J. Comp. Neurol. 178, 225–254. https://doi.org/10.1002/cne.901780204.

Krettek, J.E., Price, J.L., 1978b. A description of the amygdaloid complex in the rat and cat with observations on intra-amygdaloid axonal connections. J. Comp. Neurol. 178, 255–280. https://doi.org/10.1002/cne.901780205.

Li, H., Penzo, M.A., Taniguchi, H., Kopec, C.D., Huang, Z.J., Li, B., 2013. Experience-dependent modification of a central amygdala fear circuit. Nat. Neurosci. 16, 332–339. https://doi.org/10.1038/nn.3322.

Liang, K.C., Juler, R.G., McGaugh, J.L., 1986. Modulating effects of posttraining epinephrine on memory: involvement of the amygdala noradrenergic system. Brain Res. 368, 125–133. https://doi.org/10.1016/0006-8993(86)91049-8.

Lomarev, M., Denslow, S., Nahas, Z., Chae, J.H., George, M.S., Bohning, D.E., 2002. Vagus nerve stimulation (VNS) synchronized BOLD fMRI suggests that VNS in depressed adults has frequency/dose dependent effects. J. Psychiatr. Res. 36, 219–227. https://doi.org/10.1016/s0022-3956(02)00013-4.

Luo, Y., Zhou, J., Li, M.X., Wu, P.F., Hu, Z.L., Ni, L., et al., 2015. Reversal of aging-related emotional memory deficits by norepinephrine via regulating the stability of surface AMPA receptors. Aging Cell 14, 170–179. https://doi.org/10.1111/acel.12282.

Mathew, E., Tabet, M.N., Robertson, N.M., Hays, S.A., Rennaker, R.L., Kilgard, M.P., et al., 2020. Vagus nerve stimulation produces immediate dose-dependent anxiolytic effect in rats. J. Affect. Disord. 265, 552–557. https://doi.org/10.1016/j.jad.2019.11.090.

Natividad, L.A., Buczynski, M.W., Herman, M.A., Kirson, D., Oleata, C.S., Irimia, C., et al., 2017. Constitutive increases in amygdalar corticotropin-releasing factor and fatty acid amide hydrolase drive an anxious phenotype. Biol. Psychiatr. 82, 500–510. https://doi.org/10.1016/j.biopsych.2017.01.005.

Noble, L.J., Meruva, V.B., Hays, S.A., Rennaker, R.L., Kilgard, M.P., McIntyre, C.K., 2019. Vagus nerve stimulation promotes generalization of conditioned fear extinction and reduces anxiety in rats. Brain Stimul. 12, 9–18. https://doi.org/10.1016/j.brs.2018.09.013.

Paretkar, T., Dimitrov, E., 2019. Activation of enkephalinergic (Enk) interneurons in the central amygdala (CeA) buffers the behavioral effects of persistent pain. Neurobiol. Dis. 124, 364–372. https://doi.org/10.1016/j.nbd.2018.12.005.

Patriarchi, T., Buonarati, O.R., Hell, J.W., 2018. Postsynaptic localization and regulation of AMPA receptors and Cav1.2 by beta2 adrenergic receptor/PKA and Ca(2+)/CaMKII signaling. EMBO J. 37, e9977 https://doi.org/10.15252/embj.201899771.

Poulin, J.F., Castonguay-Lebel, Z., Laforest, S., Drolet, G., 2008. Enkephalin co-expression with classic neurotransmitters in the amygdaloid complex of the rat. J. Comp. Neurol. 506, 943–959. https://doi.org/10.1002/cne.21587.

Ricardo, J.A., Koh, E.T., 1978. Anatomical evidence of direct projections from the nucleus of the solitary tract to the hypothalamus, amygdala, and other forebrain structures in the rat. Brain Res. 153, 1–26. https://doi.org/10.1016/0006-8993(78)91125-3.

Roosevelt, R.W., Smith, D.C., Clough, R.W., Jensen, R.A., Browning, R.A., 2006. Increased extracellular concentrations of norepinephrine in cortex and hippocampus following vagus nerve stimulation in the rat. Brain Res. 1119, 124–132. https://doi.org/10.1016/j.brainres.2006.08.048.

Ruffoli, R., Giorgi, F.S., Pizzanelli, C., Murri, L., Paparelli, A., Fornai, F., 2011. The chemical neuroanatomy of vagus nerve stimulation. J. Chem. Neuroanat. 42, 288–296. https://doi.org/10.1016/j.jchemneu.2010.12.002.

Rush, A.J., George, M.S., Sackeim, H.A., Marangell, L.B., Husain, M.M., Giller, C., et al., 2000. Vagus nerve stimulation (VNS) for treatment-resistant depressions: a multicenter study. Biol. Psychiatr. 47, 276–286. https://doi.org/10.1016/s0006-3223(99)00304-2.

Samson, R.D., Pare, D., 2005. Activity-dependent synaptic plasticity in the central nucleus of the amygdala. J. Neurosci. 25, 1847–1855. https://doi.org/10.1523/JNEUROSCI.3713-04.2005.

Shackman, A.J., Fox, A.S., 2016. Contributions of the central extended amygdala to fear and anxiety. J. Neurosci. 36, 8050–8063. https://doi.org/10.1523/JNEUROSCI.0982-16.2016.

Shah, A.P., Carreno, F.R., Wu, H., Chung, Y.A., Frazer, A., 2016. Role of TrkB in the anxiolytic-like and antidepressant-like effects of vagal nerve stimulation: comparison with desipramine. Neuroscience 322, 273–286. https://doi.org/10.1016/j.neuroscience.2016.02.024.

Shen, Z.C., Wu, P.F., Wang, F., Xia, Z.X., Deng, Q., Nie, T.L., et al., 2019. Gephyrin palmitoylation in basolateral amygdala mediates the anxiolytic action of benzodiazepine. Biol. Psychiatr. 85, 202–213. https://doi.org/10.1016/j.biopsych.2018.09.024.

Silberman, Y., Winder, D.G., 2013. Corticotropin releasing factor and catecholamines enhance glutamatergic neurotransmission in the lateral subdivision of the central amygdala. Neuropharmacology 70, 316–323. https://doi.org/10.1016/j.neuropharm.2013.02.014.

Thompson, B.L., Rosen, J.B., 2006. Immediate-early gene expression in the central nucleus of the amygdala is not specific for anxiolytic or anxiogenic drugs. Neuropharmacology 50, 57–68. https://doi.org/10.1016/j.neuropharm.2005.07.024.

Tye, K.M., Deisseroth, K., 2012. Optogenetic investigation of neural circuits underlying brain disease in animal models. Nat. Rev. Neurosci. 13, 251–266. https://doi.org/10.1038/nrn3171.

Tye, K.M., Prakash, R., Kim, S.Y., Fenno, L.E., Grosenick, L., Zarabi, H., et al., 2011. Amygdala circuitry mediating reversible and bidirectional control of anxiety. Nature 471, 358–362. https://doi.org/10.1038/nature09820.

Urban, D.J., Roth, B.L., 2015. DREADDs (designer receptors exclusively activated by designer drugs): chemogenetic tools with therapeutic utility. Annu. Rev. Pharmacol. Toxicol. 55, 399–417. https://doi.org/10.1146/annurev-pharmtox-010814-124803.

Van Bockstaele, E.J., Peoples, J., Telegan, P., 1999. Efferent projections of the nucleus of the solitary tract to peri-locus coeruleus dendrites in rat brain: evidence for a monosynaptic pathway. J. Comp. Neurol. 412, 410–428. https://doi.org/10.1002/(sici)1096-9861(19990927)412:3<410::aid-cne3>3.0.co;2-f.

Ventura-Silva, A.P., Melo, A., Ferreira, A.C., Carvalho, M.M., Campos, F.L., Sousa, N., et al., 2013. Excitotoxic lesions in the central nucleus of the amygdala attenuate stress-induced anxiety behavior. Front. Behav. Neurosci. 7, 32. https://doi.org/10.3389/fnbeh.2013.00032.

Wahis, J., Baudon, A., Althammer, F., Kerspern, D., Goyon, S., Hagiwara, D., et al., 2021. Astrocytes mediate the effect of oxytocin in the central amygdala on neuronal activity and affective states in rodents. Nat. Neurosci. 24, 529–541. https://doi.org/10.1038/s41593-021-00800-0.

Watanabe, T., Nakagawa, T., Yamamoto, R., Maeda, A., Minami, M., Satoh, M., 2003. Involvement of noradrenergic system within the central nucleus of the amygdala in naloxone-precipitated morphine withdrawal-induced conditioned place aversion in rats. Psychopharmacology (Berl) 170, 80–88. https://doi.org/10.1007/s00429-018-1623-3.

Zhang, H., Li, K., Chen, H.S., Gao, S.Q., Xia, Z.X., Zhang, J.T., et al., 2018. Dorsal raphe projection inhibits the excitatory inputs on lateral habenula and alleviates depressive behaviors in rats. Brain Struct. Funct. 223, 2243–2258. https://doi.org/10.1007/s00429-018-1623-3.

Zhou, H.Y., He, J.G., Hu, Z.L., Xue, S.G., Xu, J.F., Cui, Q.Q., et al., 2019. A-kinase anchoring protein 150 and protein kinase A complex in the basolateral amygdala contributes to depressive-like behaviors induced by chronic restraint stress. Biol. Psychiatr. 86, 131–142. https://doi.org/10.1016/j.biopsych.2019.03.967.

Zhou, J., Luo, Y., Zhang, J.T., Li, M.X., Wang, C.M., Guan, X.L., et al., 2015. Propranolol decreases retention of fear memory by modulating the stability of surface glutamate receptor GluA1 subunits in the lateral amygdala. Br. J. Pharmacol. 172, 5068–5082. https://doi.org/10.1111/bph.13272.

Zhu, H., Liu, Z., Zhou, Y., Yin, X., Xu, B., Ma, L., et al., 2017. Lack of beta2-AR increases anxiety-like behaviors and rewarding properties of cocaine. Front. Behav. Neurosci. 11, 49. https://doi.org/10.3389/fnbeh.2017.00049.